Chemical Science

EDGE ARTICLE

View Article Online
View Journal | View Issue

Cite this: *Chem. Sci.*, 2015, **6**, 6572

Ligand survey results in identification of PNP pincer complexes of iridium as long-lived and chemoselective catalysts for dehydrogenative borylation of terminal alkynes†

Chun-I Lee,[a] Jessica C. DeMott,[a] Christopher J. Pell,[a] Alyson Christopher,[b] Jia Zhou,[c] Nattamai Bhuvanesh[a] and Oleg V. Ozerov*[a]

Received 15th June 2015
Accepted 3rd August 2015

DOI: 10.1039/c5sc02161h

www.rsc.org/chemicalscience

Following the report on the successful use of SiNN pincer complexes of iridium as catalysts for dehydrogenative borylation of terminal alkynes (DHBTA) to alkynylboronates, this work examined a wide variety of related pincer ligands in the supporting role in DHBTA. The ligand selection included both new and previously reported ligands and was developed to explore systematic changes to the SiNN framework (the 8-(2-diisopropylsilylphenyl)aminoquinoline). Surprisingly, only the diarylamido/bis(phosphine) PNP system showed any DHBTA reactivity. The specific PNP ligand (bearing two diisopropylphosphino side donors) used in the screen showed DHBTA activity inferior to SiNN. However, taking advantage of the ligand optimization opportunities presented by the PNP system *via* the changes in the substitution at phosphorus led to the discovery of a catalyst whose activity, longevity, and scope far exceeded that of the original SiNN archetype. Several Ir complexes were prepared in a model PNP system and evaluated as potential intermediates in the catalytic cycle. Among them, the (PNP)Ir diboryl complex and the borylvinylidene complex were shown to be less competent in catalysis and thus likely not part of the catalytic cycle.

Introduction

Selective conversion of C–H bonds into C–B bonds (Fig. 1) has attracted broad attention over the last two decades.[1,2] The resulting organoboron compounds are relatively stable, non-toxic, and can be easily transformed into C–O or C–C bonds *via* oxidation[3–6] or Suzuki–Miyaura coupling.[7–9] Many examples of alkane,[10–12] arene,[13,14] and alkene[15,16] dehydrogenative borylation, as well as benzylic[17] and allylic[18] C–H borylation have been reported. The dehydrogenative arene borylation has been proven especially fruitful with very impressive advances by Hartwig *et al.*[19,20] and Smith and Maleczka *et al.*[21,22] already finding applications.[2]

The development of C–H borylation methods did not include the C(sp)–H bonds of terminal alkynes. The products of dehydrogenative borylation of terminal alkynes (DHBTA), alkynylboronates, are versatile building blocks in synthetic chemistry. Their synthetic value derives not just from the direct use in $C–C_{alkynyl}$ coupling,[23] but more so from pursuing the reactions of the triple bond. Cyclotrimerization,[24] [3 + 2] cycloaddition,[25] cyclopentenone synthesis,[26] hydrozirconation,[27] enyne metathesis,[28] and others[29–32] have been reported; these reactions yield more complex molecules that contain C–B bonds in positions that would be difficult to borylate by alternative means.

The classical synthesis of alkynylboronates was developed by Brown *et al.*: deprotonation of alkyne by *n*-BuLi, followed by reaction with a boric ester and quench with anhydrous acid.[33] An Ag-catalyzed variation was reported in 2014 by Hu *et al.*[34] Ingleson *et al.* also recently demonstrated that certain

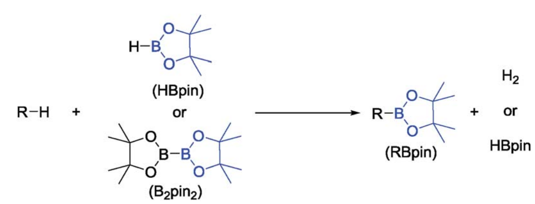

Fig. 1 C–H borylation (dehydrogenative borylation).

[a]Department of Chemistry, Texas A&M University, College Station, TX 77842, USA. E-mail: ozerov@chem.tamu.edu

[b]Department of Chemistry, Brandeis University, MS 015, 415 South Street, Waltham, MA 02454, USA

[c]Department of Chemistry, Harbin Institute of Technology, Harbin 150001, China

† Electronic supplementary information (ESI) available: Supporting information in the form of descriptions of experiments, characterization data, crystallographic information in the form of CIF files, and a video recording of hydrogen evolution from the mixture of 3-methyl-3-trimethylsiloxy-1-butyne, **17-Ir-COE** and HBpin in toluene. CCDC 1014977–1014979 and 1015119. For ESI and crystallographic data in CIF or other electronic format see DOI: 10.1039/c5sc02161h

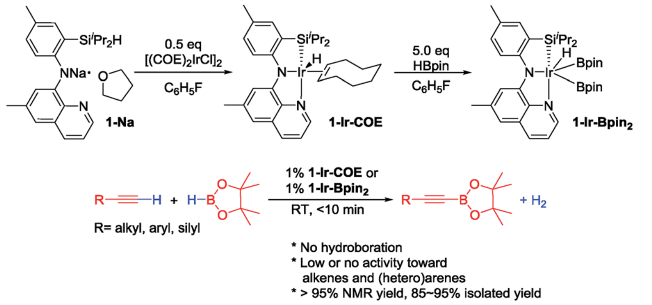

Fig. 2 Synthesis of SiNN Ir complexes (top) and DHBTA catalyzed by SiNN Ir complexes (bottom).

borenium cations can react with terminal alkynes to give alkynylboronates.[35] Just as with borylation of sp^2 and sp^3 C–H bonds, catalysis of direct coupling of a C–H bond with a B–H bond (Fig. 1 and R = alkynyl for DHBTA) carries significant advantages (if the catalysis is efficient enough): better atom economy, as well as milder conditions allowing greater functional group compatibility. In comparison to C(sp^2)–H and C(sp^3)–H bonds, for the relatively acidic C(sp)–H bonds (pK_a ~ 25) of terminal alkynes, the C–H activation itself is generally not a difficult task and C–H bond selectivity would not typically be an issue. On the other hand, in contrast to the non-olefinic C(sp^2)–H and C(sp^3)–H substrates, a combination of a triple C≡C bond, a B–H bond and a metal catalyst is very likely to lead to hydroboration.[36,37] In addition, hydrogenation[38] of the alkyne substrate or product with H_2 (the by-product of DHBTA) may also be a concern.

In 2013, we reported the first example of catalytic DHBTA performed by Ir complexes of a SiNN pincer[39] ligand (**1-Ir-COE** and **1-Ir-Bpin$_2$**, Fig. 2).[40] The reaction was strictly chemoselective and could be performed under very mild conditions (ambient temperature, *ca.* 10 turnovers per min) with a variety of alkyl-, aryl- and silyl- terminal alkynes in high yield. However, the catalyst longevity was limited to *ca.* 100 turnovers. Very recently, Tsuchimoto *et al.* described DHBTA catalysis by

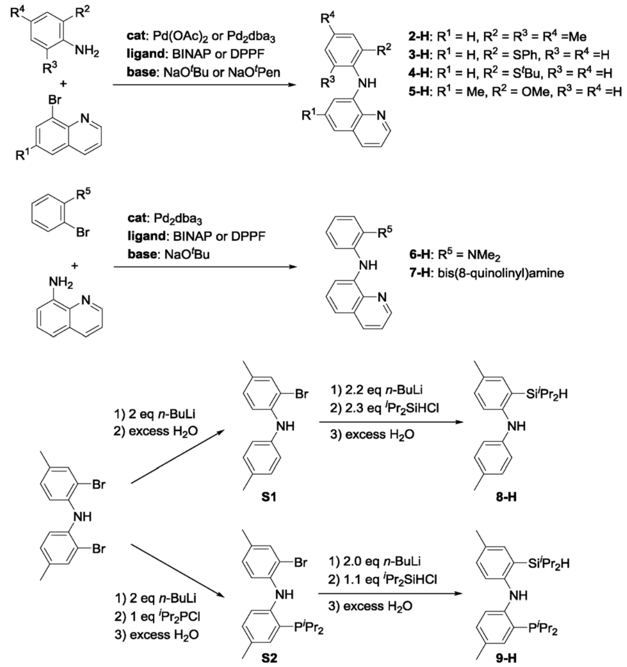

Scheme 1 Synthesis of ligands used in screening for DHBTA.

$Zn(OTf)_2$/pyridine using 1,8-nathpthalenediamidoborane.[41] The Tsuchimoto process displayed a wide scope similar to (SiNN)Ir, but operated much slower (*ca.* 1 turnover per hour) even at 100 °C. Our group also reported that (POCOP)Pd complexes are modest DHBTA catalysts for some substrates.[42]

The discovery of the prowess of the SiNN ligand in DHBTA was rather serendipitous, and we sought to explore the associated ligand space in a more systematic fashion. Here we report the exploration of a series of Ir complexes of related ligands as potential catalysts in DHBTA that has led to the discovery of a new highly active, much more long-lived catalyst with a broader scope, as well as to the insight into the role of possible intermediates in DHBTA.

Results and discussion

Synthesis and screening of ligands for DHBTA

In light of the success of **1-Ir-COE** in DHBTA, we decided to examine a series of ligands that systematically explored variations of the SiNN ligand features (Fig. 3). From **2-H** to **7-H**, we preserved the central amido donor and the quinoline fragment of SiNN but removed the silane side arm (**2-H**) or replaced it with hemilabile donors (**3-H** to **7-H**). For **8-H** and **9-H**, the silane segment and the central amido donor were maintained while

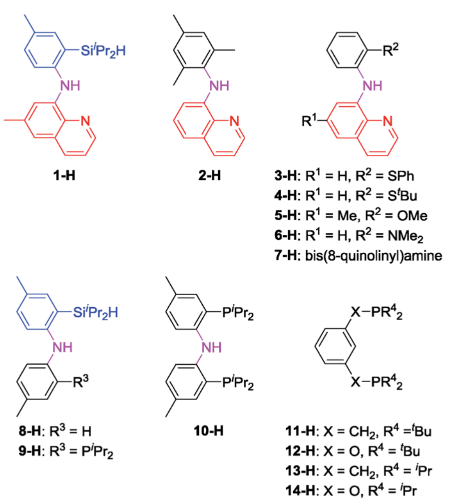

Fig. 3 Ligands selected for DHBTA screening.

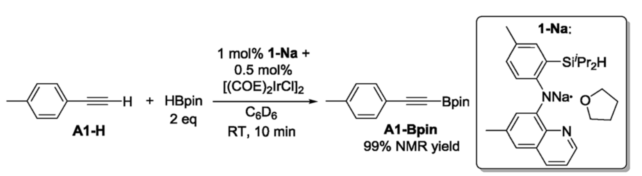

Scheme 2 DHBTA catalyzed by **1-Ir-COE** generated *in situ* from **1-Na**.

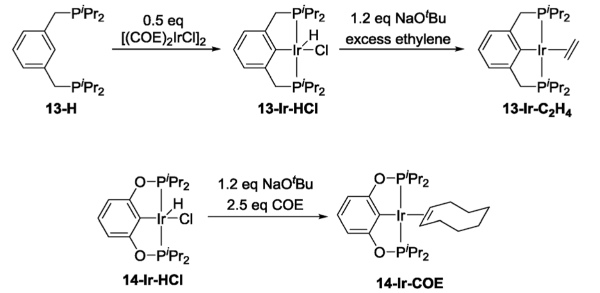

Scheme 3 Synthesis of 13-Ir-C_2H_4 and 14-Ir-COE.

the quinoline moiety was eliminated (**8-H**) or substituted with a phosphine donor (**9-H**). We also included the PNP ligand (**10-H**) and the PCP/POCOP ligands (**11-H to 14-H**) because these are commonly used pincer ligands with a rich history of C–H activation chemistry with Ir.[43–46]

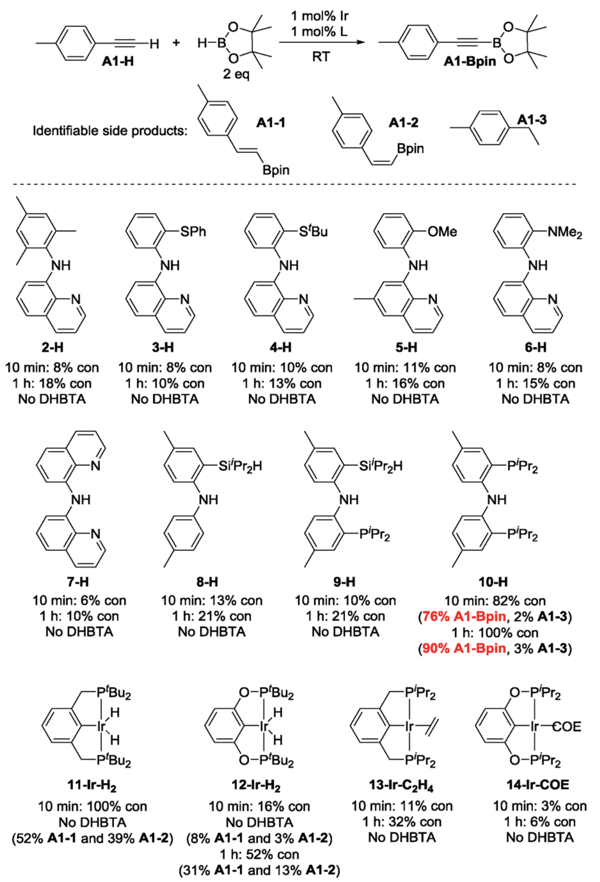

Chart 1 Ligand screening in DHBTA. For 2-H to 10-H: in the following order, the ligand (0.0010 mmol), $NaN(TMS)_2$ (0.0010 mmol), $[(COE)_2IrCl]_2$ (0.00050 mmol) and HBpin (0.20 mmol) were mixed in C_6D_6 in a J. Young tube. 4-Ethynyltoluene (0.10 mmol) was then added in 4 portions with 1 min intervals and the mixture was allowed to stand at ambient temperature for 10 min (see ESI† for details). For 11-H to 14-H: the iridium complex (0.0010 mmol) and HBpin (0.20 mmol) were mixed in C_6D_6 in a J. Young tube. 4-ethynyltoluene (0.10 mmol) was then added in 4 portions with 1 min intervals and the mixture was allowed to stand at ambient temperature for 10 min (see ESI† for details). The numbers for "% con" refer to the conversion of A1-H.

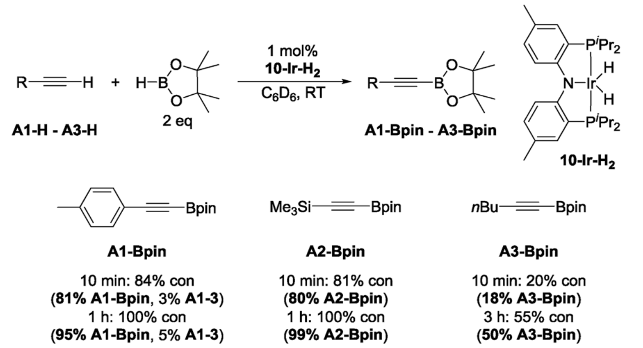

Chart 2 DHBTA catalyzed by 10-Ir-H_2.

The syntheses of ligands used in the screening of DHBTA are shown in Scheme 1. Quinoline derivatives (*i.e.* **2-H**,[47] **3-H**, **4-H**, **5-H**, **6-H**,[48] **7-H**[48]) were readily synthesized *via* Buchwald–Hartwig coupling of 8-bromoquinoline with various anilines or 8-aminoquinoline with various bromoarenes. **8-H** was prepared *via* the intermediate **S1**. The synthesis of **S1** relied on the same selective dilithiation of bis(2-bromo-4-methylphenyl)amine we previously used in the synthesis of **S2**,[49,50] followed by quenching with water. Pure **S1** was isolated in 86% yield by column chromatography. Treatment of **S1** with *n*-BuLi, followed by addition of $^iPr_2SiHCl$ and workup gave **8-H** in 73% yield. The new SiNP ligand **9-H** was prepared from **S2** through a similar protocol.

In our original DHBTA report,[40] we demonstrated that generation of the **1-Ir-COE** precatalyst *in situ* from **1-Na** and $[(COE)_2IrCl]_2$ (Scheme 2) produced results equivalent to those obtained using isolated **1-Ir-COE**. Therefore, we used a similar synthetic approach here for testing catalysis using the series of ligands with central amido donors (**2-H** to **10-H**). They were deprotonated with 1 equiv. of $NaN(SiMe_3)_2$ *in situ*, allowed to react with 0.5 equiv. of $[(COE)_2IrCl]_2$ in C_6D_6 and the resultant solutions were tested for catalytic DHBTA activity. In the case of PCP/POCOP ligands **11–14**, we isolated dihydride complexes (**11-Ir-H$_2$**[51] and **12-Ir-H$_2$**[52]) or alkene complexes (**13-Ir-C$_2$H$_4$** and **14-Ir-COE**) to be used in DHBTA testing.

The precatalyst **13-Ir-C$_2$H$_4$** was obtained after modification of previously reported procedures for related compounds (Scheme 3, top).[53–55] Thermolysis of **13-H** with $[(COE)_2IrCl]_2$ at 80 °C overnight in toluene resulted in a dark red solution that contained *ca.* 85% of the desired product (^{31}P NMR evidence). Column chromatography allowed for the collection of 99% pure **13-Ir-HCl** in 22% yield. This portion of **13-Ir-HCl** was then treated with a slight excess of NaO^tBu in toluene, degassed, and then stirred under an atmosphere of ethylene for 30 min. After filtration and removal of volatiles under vacuum, analytically pure **13-Ir-C$_2$H$_4$** was obtained as a dark brown solid in 66% isolated yield (based on **13-Ir-HCl**). **14-Ir-COE** was synthesized by reacting the previously reported **14-Ir-HCl**[56,57] with a slight excess of NaO^tBu and COE in C_6D_6 (Scheme 3, bottom).

4-Ethynyltoluene (**A1-H**) was selected as the alkyne for testing. We mimicked the conditions that were successful for the SiNN ligand **1**, with 1 mol% Ir loading and 2 equiv. of HBpin

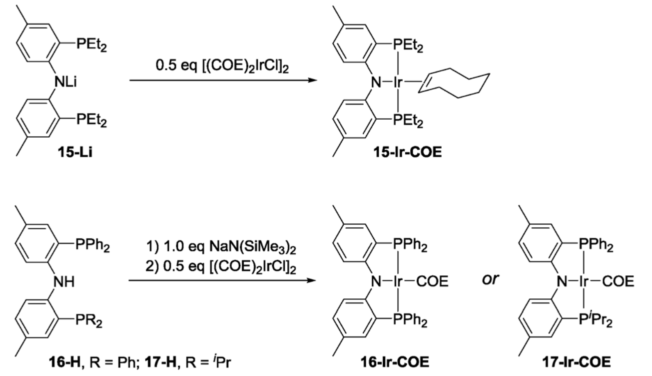

Scheme 4 Synthesis of (PNP)Ir(COE) complexes.

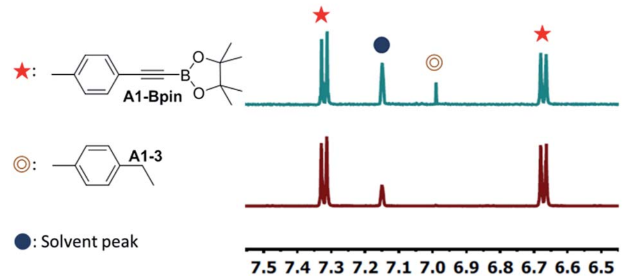

Fig. 4 Partial ^{1}H NMR spectra of DHBTA reaction mixtures catalyzed by (a) 1 mol% **15-Ir-COE** (entry 3 in Table 1) and (b) 1 mol% **1-Ir-COE** (entry 1 in Table 1).

used at ambient temperature in C_6D_6 solvent. The results are summarized in Chart 1. Surprisingly, of all the ligands tested, only **10-H** showed any DHBTA reactivity. In all other cases, no evidence for the DHBTA product **A1-Bpin** was visible by ^{1}H NMR spectroscopy after 1 h. In general, sluggish and nonselective hydrogenation and hydroboration was observed for **2-H** to **9-H**, and for the iso-propyl PCP/POCOP iridium complexes (**13-Ir-C_2H_4** and **14-Ir-COE**). For *tert*-butyl PCP/POCOP iridium complexes (**11-Ir-H_2** and **12-Ir-H_2**), a mixture of *trans*-alkenylboronate (**A1-1**) and *cis*-alkenylboronate (**A1-2**) were observed as major products. The use of **10-H** resulted in 76% **A1-Bpin** after 10 min and 90% (NMR evidence) after 1 h, with about 3% of 4-ethyltoluene (**A1-3**, from apparent hydrogenation of **A1-H**). We also tested one of the most active arene borylation catalyst systems ([(COD)Ir(OMe)]$_2$ + 4,4′-di-*tert*-butyl-bipyridine)[58] but no catalysis of any kind was observed after 1 h at RT.[59] It is difficult to rationalize the results of the ligand screen other than to cautiously note that a central amido donor may be crucial and that selectivity for DHBTA is quite sensitive to the balance of steric and electronic factors.

With this lead in hand, we tested isolated **10-Ir-H_2**[59] as a catalyst in reactions with 4-ethynyltoluene (**A1-H**), trimethylsilylacetylene (**A2-H**), and 1-hexyne (**A3-H**) (Chart 2). The effectiveness of **10-Ir-H_2** in the DHBTA of 4-ethynyltoluene (**A1-H**) was similar to the catalyst generated from **10-H** *in situ*. DHBTA of trimethylsilylacetylene (**A2-H**) was finished in 1 h and gave an excellent yield of **A2-Bpin**. The catalytic activity of **10-Ir-H_2** towards **A3-H** was significantly lower than towards **A1-H** and **A2-H** and only 50% yield was achieved after 3 h. A small amount of the hydrogenation product **A1-3** was observed in DHBTA of **A1-H**, but no hydrogenation products were detected in the reactions of **A2-H** and **A3-H**.

Table 1 Catalytic results for DHBTA using various PNP Ir complexes and **1-Ir-COE**[a]

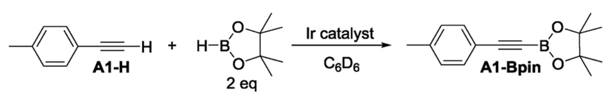

#	Catalyst	[Ir] mol%	Time	Con (%)	Yield (%)	A1-3 (%)
1	**1-Ir-COE**	1	10 min	100	99	0
2	**10-Ir-H_2**	1	1 h	100	95[b]	5
3	**15-Ir-COE**	1	10 min	100	97	2
4	**16-Ir-COE**	1	10 min	27	21	2
5	**17-Ir-COE**	1	10 min	100	97	2
6	**1-Ir-COE**	0.25	1 h	44	43[c]	0
7	**10-Ir-H_2**	0.25	4 h	100	90[d]	6
8	**15-Ir-COE**	0.25	2 h	100	82[e]	5
9	**17-Ir-COE**	0.25	10 min	100	92	2
10	**17-Ir-COE**	0.05	2 h	100	85	7
11	**17-Ir-COE**	0.025	8 h	100	85[f]	9
12	**17-Ir-COE**	0.025	1 h[g]	100	84	10
13	**17-Ir-COE**	0.01	2 h[g]	77	65	5

[a] The iridium complex and HBpin (0.20 mmol) were mixed in C_6D_6 in a J. Young tube. **A1-H** (0.10 mmol) was then added in 4 portions with 1 min intervals and the mixture was allowed to stand at ambient temperature (see ESI for details). [b] 10 min: 81% yield. [c] 10 min: 37% yield. [d] 10 min: 34% yield. [e] 10 min: 45% yield. [f] 10 min: 13% yield. [g] Run at 60 °C.

Testing of (PNP)Ir complexes with various phosphine substituents

The effectiveness of **10-Ir-H_2** fell somewhat short of the SiNN-based catalysis, where >95% yield of **A1/2/3-Bpin** was obtained in <10 min and without any hydrogenation side products. Nonetheless, we were encouraged by the results because the PNP framework offers facile opportunities for optimization of the ligand *via* substituent variation. We selected previously reported PNP ligands **15-H**,[50] **16-H**,[60] and **17-H**[50,61] for further testing in DHBTA. The syntheses of the corresponding Ir-COE complexes are depicted in Scheme 4. **15-H** is an oil that is difficult to purify; however, the Li derivative (**15-Li**) could be isolated in in 56% yield as a pure solid. **15-Li** was then reacted with 0.5 equiv. of [(COE)$_2$IrCl]$_2$ to yield **15-Ir-COE**. **16-Ir-COE**[62] and **17-Ir-COE** were synthesized *via* one-pot reactions by deprotonation of the neutral ligands *in situ* and treatment with [(COE)$_2$IrCl]$_2$.

The newly synthesized and isolated (PNP)Ir(COE) complexes (**15-Ir-COE, 16-Ir-COE, 17-Ir-COE**), **10-Ir-H_2**, and the previously reported **1-Ir-COE** were all tested in DHBTA by using **A1-H** as the substrate with 2 equiv. of HBpin at ambient temperature in C_6D_6 solvent. The results are summarized in Table 1. At 1 mol% catalyst loading, **15-Ir-COE, 17-Ir-COE, 10-Ir-H_2**, as well as **1-Ir-**

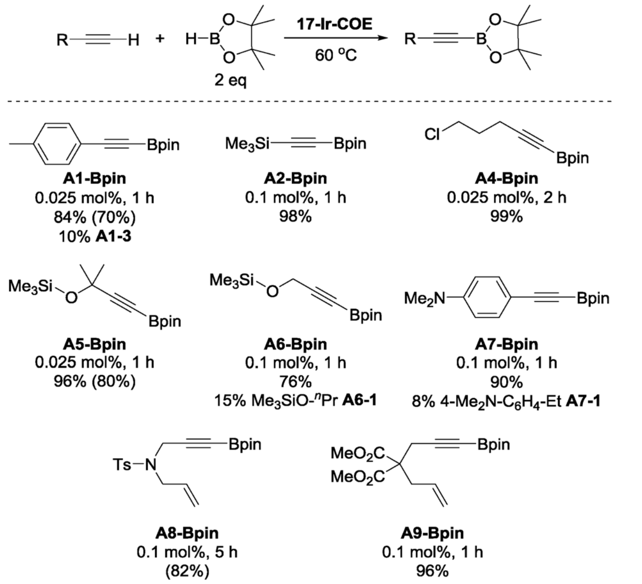

Chart 3 DHBTA of representative terminal alkynes catalyzed by 17-Ir-COE. [a] 17-Ir-COE and HBpin (0.20 mmol) were mixed in C_6D_6 in a J. Young tube. Alkyne (0.10 mmol) was then added in 4 portions with 1 min intervals at RT and the mixture was heated at 60 °C (see ESI† for details). [b] NMR yield. [c] Yields in parentheses are isolated yields in preparative-scale (10 mmol alkyne) reactions that used toluene or fluorobenzene as solvent instead of C_6D_6.

COE gave excellent yields of **A1-Bpin** at ambient temperature, whereas **16-Ir-COE** did not (entry 4) and was eliminated from further consideration. At 0.25% Ir, **17-Ir-COE** showed superior reactivity to **1-Ir-COE, 10-Ir-H$_2$**, and **15-Ir-COE** by producing 92% **A1-Bpin** in 10 min. **1-Ir-COE** gave 43% yield after 1 h (entry 6) and the yield did not increase with longer reaction times, suggesting faster catalyst decomposition for the SiNN-based catalyst. **17-Ir-COE** was able to effect 100% conversion of **A-1H** and 85% yield of **A1-Bpin** (NMR evidence) even at 0.025% loading in only hours at ambient temperature. The reaction rate was higher at 60 °C (entry 12) without loss in yield. The 84% yield of **A1-Bpin** at 0.025 mol% catalyst loading (entry 12) corresponds, impressively, to 3400 turnovers. Under incomplete conversion with 0.01 mol% loading (entry 13), a turnover number of 6500 was achieved after 2 h at 60 °C. In terms of chemoselectivity, **1-Ir-COE** is superior in DHBTA of **A1-H** as it gave **A1-Bpin** as the product exclusively; 2–10% of hydrogenation product **A1-3** was observed in all reactions catalyzed by the (PNP)Ir complexes (Fig. 4). Because **15** and **17** gave faster catalysis than **10**, it is possible that a less sterically encumbered ligand is advantageous. The lower reactivity of **16** may in turn reflect sensitivity to the electronic factors.

To further explore the catalytic reactivity of **17-Ir-COE, A1-H, A2-H**, 5-chloro-1-pentyne (**A4-H**), as well as 3-methyl-3-trimethylsiloxy-1-butyne (**A5-H**), trimethylsilyl propargyl ether (**A6-H**), 4-dimethylamino-phenylacetylene (**A7-H**), *N*-tosylated allyl propargyl amine (**A8-H**), and dimethyl 2-allyl-2-(prop-2-yn-1-yl) malonate (**A9-H**) were chosen as representative substrates for aromatic, silyl, aliphatic terminal alkynes, propargyl derivatives and 1,6-enynes, respectively (Chart 3). For **A1-H**, 84% NMR yield

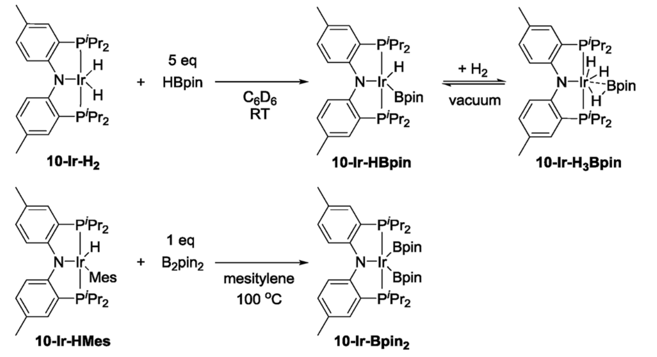

Scheme 5 The synthesis of 10-Ir-HBpin and its equilibrium with 10-Ir-H$_3$Bpin (top). The synthesis of 10-Ir-Bpin$_2$ (bottom).

was observed and accompanied with 10% hydrogenation product **A1-3**; similar results were obtained with **A6-H** and **A7-H.** 96–99% NMR yields were obtained for **A2-, A4-, A5**, and **A9-Bpin** with 0.025 to 0.1 mol% loading of **17-Ir-COE** as the catalyst. Borylation of **A2-H** and **A6-H** was also performed with reduced amount of HBpin (1.1 eq.) and comparable yields/side product (**A6-1** for **A6-H**) were obtained. No DHBTA products were observed for phenyl propargyl sulfide, 3-ethynylpyridine, 4-cyano-1-butyne, 3,3-diethoxy-1-propyne, and methyl propiolate with 0.1 mol% **17-Ir-COE. A1-Bpin, A5-Bpin** and **A8-Bpin** could be easily purified by recrystallization and were isolated in good yields in preparative-scale reactions. In contrast, **1-Ir-COE** requires 1% loading for high yields of **A1-, A2-, A4-**, and **A5-Bpin**, and is altogether ineffective for the synthesis of propargyl derivatives **A6-** and **A8-Bpin** (<10% yield at 1% catalyst loading). A mercury drop test[63] was performed with 0.025 mol% **17-Ir-COE** loading and **A1-H** as substrate. No significant yield changes were observed for either **A1-Bpin** or the major side-product **A1-3** which suggested that the catalysis is homogeneous.

Synthesis of plausible DHBTA intermediates

In order to gain new insight into the reaction mechanism, we set out to examine conceivable intermediates in DHBTA. Because of its NMR-friendly C_{2v}-symmetric structure, and because a number of its iridium complexes are already known,[44–46] we opted for ligand **10** for this study. We were particularly interested in determining the possible products

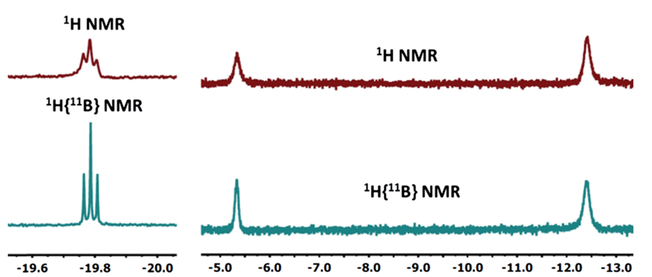

Fig. 5 The upfield region of ^1H and $^1H\{^{11}B\}$ NMR spectrum (400 MHz, C_6D_6) of 10-Ir-HBpin (left) and 10-Ir-H$_3$Bpin (right).

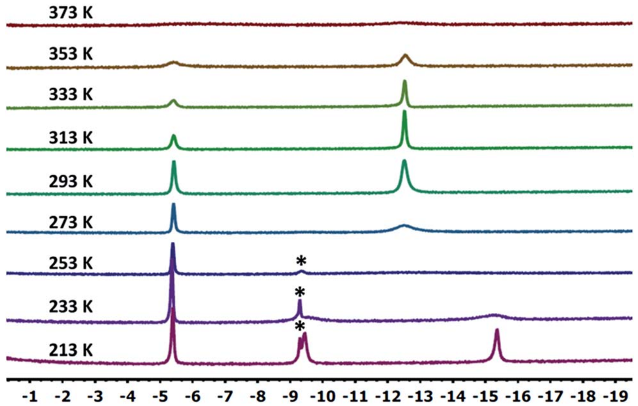

Fig. 6 Partial (upfield region) ^{1}H NMR spectrum (500 MHz, toluene-d_8) of **10-Ir-H$_3$Bpin** as a function of temperature. Small amount of unidentified impurity (marked with asterisks) was shown near −9.2 ppm.

arising from combining the **10-Ir** fragment with HBpin, terminal alkynes, and alkynylboronates and their catalytic competence.

In our report on the DHBTA activity of SiNN-based catalysts, we showed that the iridium diboryl complex **1-Ir-Bpin$_2$** can be synthesized by reacting **1-Ir-COE** with 5 equivalents of HBpin,[40] and that isolated **1-Ir-Bpin$_2$** exhibited the same catalytic activity as **1-Ir-COE.** Treating **10-Ir-H$_2$** with 5 equivalents of HBpin, however, led to a mixture of **10-Ir-H$_3$Bpin** and **10-Ir-HBpin** in equilibrium with free H_2 (top, Scheme 5). To access **10-Ir-Bpin$_2$**, we employed an alternative route of heating **10-Ir-HMes**, a good synthon for **10-Ir**,[45] with 1 equiv. of B_2pin_2. This permitted isolation of **10-Ir-Bpin$_2$** in 83% yield (bottom, Scheme 5).

10-Ir-HBpin exhibited an upfield signal at −19.8 ppm (t, $J_{P\text{-}H}$ = 8.4 Hz, 1H) in its ^{1}H NMR spectrum, and the peak sharpened upon ^{11}B decoupling (Fig. 5, left) which suggested that this proton interacted with a boron atom of the boryl. **10-Ir-H$_3$Bpin** displayed two broad upfield signals at −5.3 (1H, $\omega_{1/2}$ = 60 Hz) and −12.4 (2H, $\omega_{1/2}$ = 64 Hz) ppm in the ^{1}H NMR spectrum at ambient temperature. The resonance at −5.3 ppm ($\omega_{1/2}$ = 35 Hz) sharpened upon ^{11}B decoupling (Fig. 5, right), but the width of the peak at −12.4 ppm remained unchanged, indicating that only the proton associated with the resonance at −5.3 ppm displayed substantial coupling to the boron nucleus. The −12.4 ppm signal of **10-Ir-H$_3$Bpin** resolved into two distinct resonances (−9.43, −15.35 ppm, Fig. 6) upon cooling to 213 K. On the basis of the ^{1}H{^{11}B} and VT ^{1}H NMR spectroscopic data, **10-Ir-H$_3$Bpin** is best described as an *exo*-σ-borane dihydride complex, similarly to **12-Ir-H$_3$Bpin** in the study by Goldberg and Heinekey.[64]

Reactions of **10-Ir-H$_2$** or **10-Ir-HMes** with one equivalent or excess of **A1-H** under various conditions all led to mixtures of unidentified products that have resisted our attempts at isolation and separation. The phenomenon might be related to the fact that Rh analog **10-Rh-H$_2$** has been shown to be an alkyne dimerization catalyst[65] and PCP/POCOP iridium complexes reacted with alkynes to form a variety of allene or enyne complexes.[66,67]

For the 1 : 1 combination of **10-Ir** with **A1-Bpin**, we used DFT calculations (M06/SDD/6-311G(d,p) level of theory, see details in ESI†) to evaluate the relative thermodynamic stability of the three conceivable isomeric structures: the alkynylboronate π-complex **10-Ir-p-tol**; the vinylidene complex **10-Ir-v-tol**; and the alkynyl boryl complex **10-Ir-ynlBpin-tol** (Fig. 7). **10-Ir-v-tol** was calculated to be the lowest energy isomer, with **10-Ir-p-tol** and **10-Ir-ynlBpin-tol** lying 3.4 and 7.7 kcal mol^{-1} higher in energy, respectively.

Mixing **10-Ir-HMes** with one equivalent of **A1-Bpin** at ambient temperature overnight led to two products which appeared at 43.9 (5%) and 25.6 (11%) ppm respectively in the ^{31}P{^{1}H} NMR spectrum (Scheme 6). Further heating the mixture

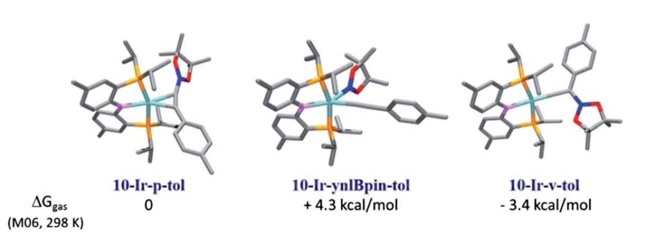

Fig. 7 Relative free energies (DFT calculation) of three possible isomers of [10-Ir + A1-Bpin].

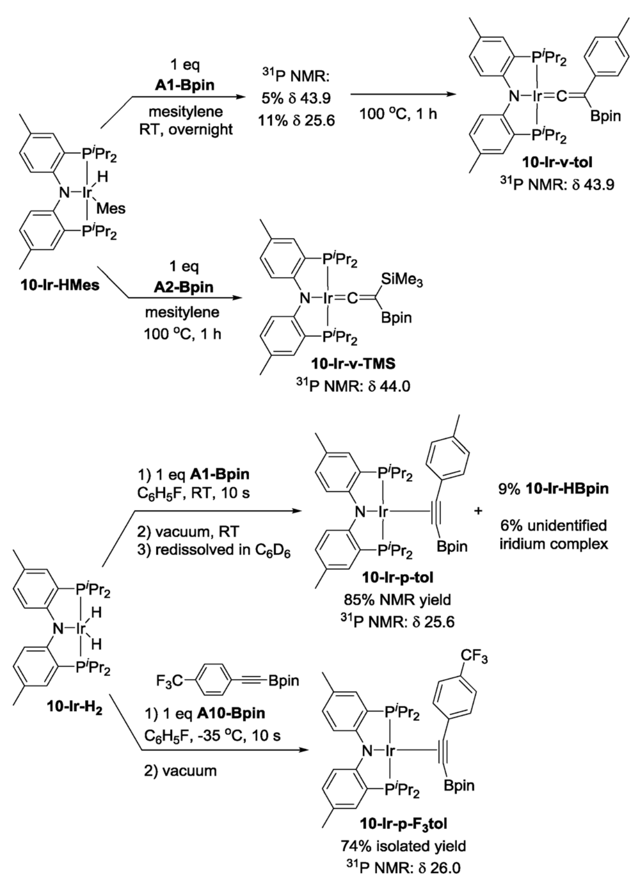

Scheme 6 Synthesis of vinylidene complexes 10-Ir-v-tol and 10-Ir-v-TMS, and *p*-alkyne complexes 10-Ir-p-tol and 10-Ir-p-F$_3$tol.

at 100 °C for 1 h cleanly converted all iridium complexes to a single product that resonated at 43.9 ppm in the ^{31}P NMR spectrum, which was isolated and identified as **10-Ir-v-tol**. The Me_3Si-substituted vinylidene analog **10-Ir-v-TMS** was also characterized by NMR spectroscopy in solution by using **A2-Bpin** as the reactant (Scheme 6). The vinylidene resonances were observed at 282.8 and 269.3 ppm in the ^{13}C NMR spectrum as expected for **10-Ir-v-tol** and **10-Ir-v-TMS**, respectively.[68] These results are consistent with the DFT prediction of **10-Ir-v-tol** as the thermodynamically favored isomer.

Esteruelas and López[69] were able to monitor the conversion of osmium boryl alkynyl complexes to vinylideneboronate esters, and we envisaged that other isomers of **10-Ir-v-tol** might be obtained if a suitable (^{Me}PNP^{iPr})Ir precursor was reacted with **A1-Bpin** under milder conditions. We first attempted to mix **10-Ir-H$_2$** with **A1-Bpin** with subsequent rapid removal of volatiles. The residue was redissolved in C_6D_6 and analyzed by ^{1}H and ^{31}P NMR spectroscopy. The major product was assigned as the alkynylboronate π-complex **10-Ir-p-tol** (Scheme 6), and its resonance in the ^{31}P NMR spectrum appeared at 25.6 ppm, which was identical to the observed intermediate in the synthesis of **10-Ir-v-tol**. We also observed 9% of **10-Ir-HBpin** formation indicating that C_{sp}–B bond cleavage is facile; the amount of **10-Ir-HBpin** increased over time. The assignment of **10-Ir-p-tol** was supported by the considerable downfield shift (8.28 ppm) of the ^{1}H NMR resonances of the *ortho*-hydrogens of the *p*-tolyl group in the coordinated **A1-Bpin**. Such downfield chemical shift is characteristic of internal aromatic alkyne π-complexes.[67,70,71] However, the isomerization from **10-Ir-p-tol** to **10-Ir-v-tol** proceeded at an appreciable rate at ambient temperature (about 50% after 15 h) and precluded the isolation of pure **10-Ir-p-tol**. We surmised that a more electron-poor alkyne should be thermodynamically less predisposed to form a vinylidene,[68] and that the alkyne isomer may also be kinetically more long-lived. To this end, we replaced **A1-Bpin** with **A10-Bpin** as the reactant (Scheme 6) and mixed it with pre-cooled **10-Ir-H$_2$** at −35 °C. We were able to isolate **10-Ir-p-F$_3$tol** as a pure red-orange solid in 74% yield. To the best of our knowledge, this is the first alkynylboronate π-complex that has been isolated and characterized. ^{31}P NMR spectroscopic analysis showed a singlet at 26.1 ppm, which was similar to that of **10-Ir-p-tol.** Consistent with our proposal, the conversion of **10-Ir-p-F$_3$tol** to the vinylidene complex **10-Ir-v-F$_3$tol** is significantly slower (about 5% after 15 h at ambient temperature) than the analogous transformation of **10-Ir-p-tol**. Similarly to **10-Ir-p-tol**, the aromatic proton signals of the 2,6-positions on **A10-Bpin** in **10-Ir-p-F$_3$tol** were shifted downfield to 8.22 ppm in the ^{1}H NMR spectrum. In the ^{13}C NMR spectrum, the carbon signal of alkynyl–C ($\underline{C}$≡C–B) in **10-Ir-p-F$_3$tol** (δ 105.7) was slightly downfield of that in free **A10-Bpin**, as expected[72] for a two-electron donor alkyne.

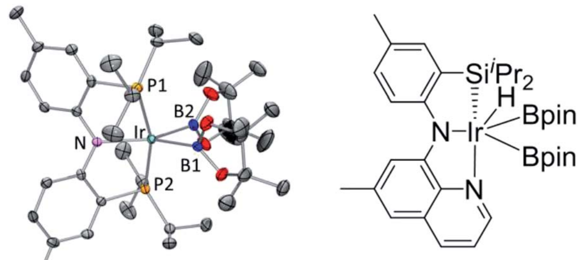

10-Ir-Bpin$_2$ **1-Ir-Bpin$_2$**

	10-Ir-Bpin$_2$	1-Ir-Bpin$_2$
Ir-B	2.034(4), 2.048(4)	2.062(6), 2.069(5)
Ir-N$_{(amido)}$	2.078(3)	2.073(4)
N$_{(amido)}$-Ir-B	144.1(1), 147.1(1)	146.2(2), 147.0(2)
B-Ir-B	68.2(2)	66.5(2)

Fig. 9 ORTEP drawing[75] (50% probability ellipsoids) of **10-Ir-Bpin$_2$** (top left) showing selected atom labeling and depiction of **1-Ir-Bpin$_2$** (top right). Hydrogen atoms are omitted for clarity in the ORTEP drawing. The selected bond distances (Å) and angles (deg) for **10-Ir-Bpin$_2$** and **1-Ir-Bpin$_2$** are summarized in the table at bottom.

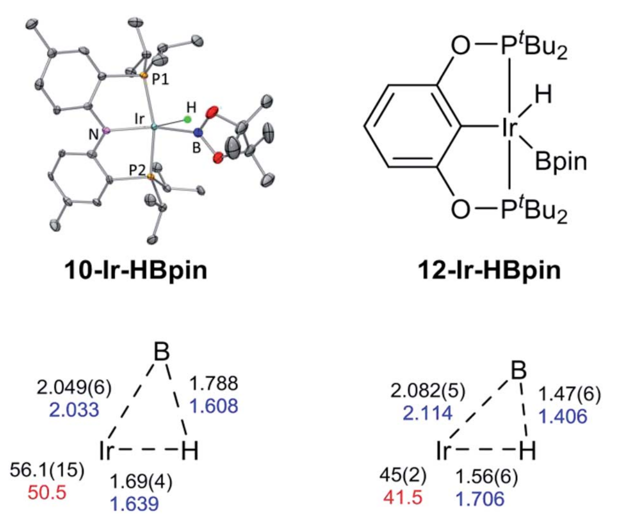

Fig. 8 ORTEP drawing[75] (50% probability ellipsoids) of **10-Ir-HBpin** (top left) showing selected atom labeling, and depiction of **12-Ir-HBpin** (top right). Hydrogen atoms are omitted for clarity in the ORTEP drawing, except for the hydride on the Ir atom. Metric parameters in the Ir/B/H triangles in compounds **10-Ir-HBpin** (bottom left) and **12-Ir-HBpin**[64] (bottom right): DFT calculated distances (Å) in blue, B–Ir–H angles (°) in red, XRD-determined distances (Å) and B–Ir–H angles (°) in black.

Select X-ray and computational structural studies

We were able to determine molecular structures of **10-Ir-HBpin**, **10-Ir-Bpin$_2$**, **10-Ir-v-tol**, and **10-Ir-p-F$_3$tol** in the solid state by X-ray diffractometry on corresponding single crystals. The structure of **10-Ir-HBpin** (Fig. 8, top left) can be compared against the analogous POCOP complex **12-Ir-HBpin**[64] (Fig. 8, top right) reported by Heinekey *et al.* **10-Ir-HBpin** is Y-shaped five-coordinate if viewed as a hydride boryl complex. To reinforce the X-ray studies, especially with respect to the location of the Ir–*H*, density functional theory (DFT) analysis of **10-Ir-HBpin** and **12-Ir-HBpin** in the gas phase using the M06 functional was also performed. DFT calculations show **10-Ir-HBpin** possesses

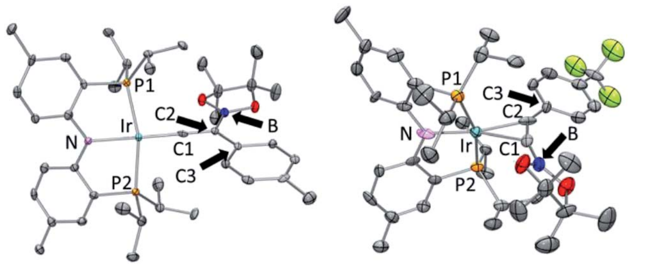

Fig. 10 ORTEP drawings[75] (50% probability ellipsoids) of **10-Ir-v-tol** (left) and **10-Ir-p-F$_3$tol** (right) showing selected atom labeling and hydrogen atoms are omitted for clarity. For **10-Ir-v-tol**, one of two molecules in the asymmetric unit is shown, and a non-coordinated fluorobenzene molecule is omitted for **10-Ir-p-F$_3$tol**. Selected bond distances (Å) and angles (deg) for **10-Ir-v-tol**: Ir–C1, 1.807(4); C1–C2, 1.334(5); P1–Ir–P2, 164.84(3); C2–C1–Ir, 178.2(3); C1–C2–C3, 120.1(3); C1–C2–B 113.1(3); C3–C2–B, 126.8(3). Selected bond distances (Å) and angles (deg) for **10-Ir-p-F$_3$tol**: Ir–C1, 2.165(11); Ir–C2, 2.101(12); C1–C2, 1.301(15); P2–Ir–P1, 163.81(10); C1–C2–C3, 147.5(11); B–C1–C2, 161.9(11).

shorter Ir–B and Ir–H bond distances and a B–H bond distance 0.2 Å longer than **12-Ir-HBpin** which was judged to be a σ-borane complex, suggesting greater degree of B–H bond activation in **10-Ir-HBpin**. The structure of **10-Ir-Bpin$_2$** (Fig. 9, top left) can be described as Y-shaped five-coordinate where the Y is defined by $N_{(amido)}$ and the two boryls with an acute B–Ir–B angle (68.2°). The Y-shaped geometry is expected for a five-coordinate d^6 complex[73,74] when the equatorial plane contains a single good π-donor ($N_{(amido)}$) and two strong σ-donors (two boryls). The two Ir-bound Bpin fragments display essentially the same metrics, and the associated **Ir–B** distances are similar to the analogous **Ir–Bpin** distances reported in the literature (2.02–2.07 Å).[13,40] In general, all parameters of bond distances and bond angles in the $NIrB_2$ plane are very close to the previously reported **1-Ir-Bpin$_2$** (Fig. 9, top right).[40] The B⋯B distance of 2.29 Å is too long for boron–boron interaction, thus **10-Ir-Bpin$_2$** should be unambiguously viewed as an Ir(III) diboryl complex.

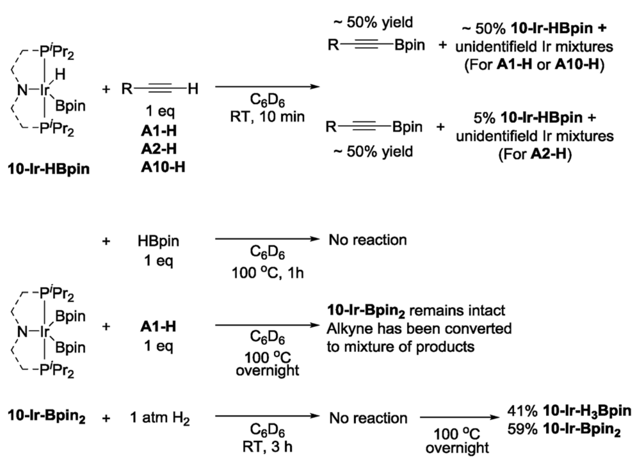

Scheme 7 Boryl transfer from **10-Ir-HBpin** to terminal alkynes (top) and reactivity of **10-Ir-Bpin$_2$**.

The coordination environment about Ir in the structures of **10-Ir-v-tol** and **10-Ir-p-F$_3$tol** (Fig. 10) can be described as distorted square planar, with the greatest deviation corresponding to the P–Ir–P angles constrained by the pincer ligand. The C2–C1–Ir bond angle (178.2(3)°) in **10-Ir-v-tol** is very close to 180° which is typical for a vinylidene complex.[68] The Ir–C1 and C1–C2 bond lengths of 1.807(4) and 1.334(5) Å, respectively, are similar to the analogous distances in the $[(Ph_2PCH_2SiMe_2)_2N]Ir{=}C{=}CH_2$ vinylidene complex reported by Fryzuk.[76] In the structure of **10-Ir-p-F$_3$tol**, **A10-Bpin** is bound to iridium in an η^2 fashion (Ir–C1: 2.165(11) Å, Ir–C2: 2.101(12) Å) and the Ir–C distances are within the range of other square planar Ir(I) alkyne complexes.[67,77,78] Both the elongation of C≡C bond (1.304 Å) and the bending of C≡C–C_{ipso} (147.5(11)°) and C≡C–B (161.9(11)°) away from 180° indicate back-donation from the iridium center to the π* orbitals of C≡C bond.[72,79]

Stoichiometric reactions of (^{Me}PNP^{iPr})Ir complexes

To examine the possible roles that four new isolated (^{Me}PNP^{iPr}) Ir complexes played in DHBTA, these compounds were examined in reactions with the three components in DHBTA: a terminal alkyne (substrate), HBpin (substrate), and H_2 (by-product). **10-Ir-HBpin** was reacted with three different terminal alkynes to study the boryl transfer ability: **A1-H**, **A2-H** and **A10-H** (Scheme 7, top). After 10 min at ambient temperature, approximately 50% yield of the corresponding alkynylboronate was observed in the ^{1}H NMR spectrum for each of the three substrates. The amount of alkynylboronate did not increase with longer reaction times; however, multiple side reactions including hydrogenation occurred. By ^{31}P NMR spectroscopic analysis, different degrees of unreacted **10-Ir-HBpin** were observed along with multiple phosphorus-containing species formed, but they could not be assigned at this stage. Surprisingly, **10-Ir-Bpin$_2$** was inert to all three major components in

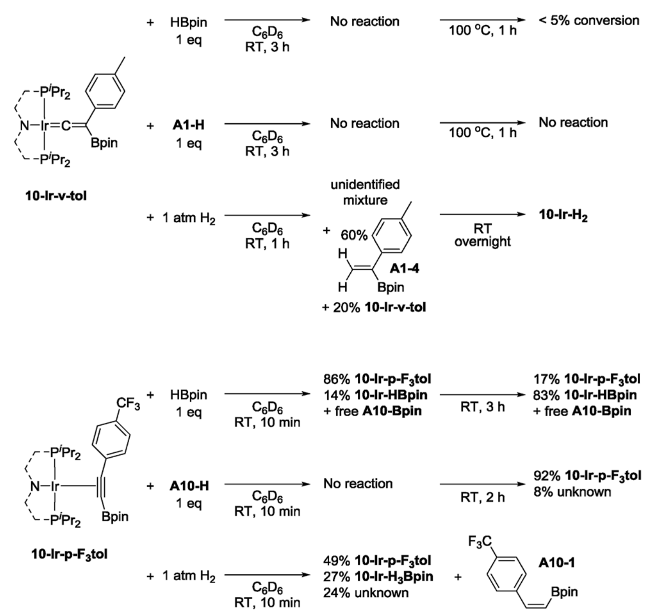

Scheme 8 Reactivity of **10-Ir-v-tol** (top) and **10-Ir-p-F$_3$tol** (bottom).

DHBTA: HBpin, terminal alkyne and H_2 (Scheme 7, bottom) in stoichiometric reactions at ambient temperature. ^{31}P NMR spectroscopic analysis showed **10-Ir-Bpin$_2$** was the only observable phosphorus-containing compound in each reaction mixture. Even at 100 °C, **10-Ir-Bpin$_2$** remained ostensibly intact in reactions with **A1-H** and HBpin. Only heating of **10-Ir-Bpin$_2$** under 1 atm H_2 at 100 °C overnight led to 41% **10-Ir-H$_3$Bpin** formation.

10-Ir-v-tol was stable toward both HBpin and **A1-H** at ambient temperature (Scheme 8, top). On the other hand, treating **10-Ir-v-tol** with H_2 quickly resulted in 80% conversion and the formation of 60% *gem*-alkenylboronate (**A1-4**) and unidentified iridium compounds in 1 h at ambient temperature. After overnight, **10-Ir-H$_2$** was the only observable species by ^{31}P NMR spectroscopic analysis. Lack of observation of **A1-4** in catalytic reaction mixtures suggested that **10-Ir-v-tol** is not present in significant concentrations during catalysis. Treating **10-Ir-p-F$_3$tol** with 1 equivalent of HBpin at ambient temperature cleanly led to 83% **10-Ir-HBpin** formation after 3 h (Scheme 8, bottom); meanwhile, equal amount of free **A10-Bpin** was observed in the ^{1}H NMR spectrum. The reaction between **10-Ir-p-F$_3$tol** and **A10-H** was relatively sluggish with no noticeable change after 10 min, and only resulted in 8% conversion after 2 h at ambient temperature based on analysis by ^{31}P NMR spectroscopy. Exposing **10-Ir-p-F$_3$tol** to 1 atm H_2 quickly yielded 27% **10-Ir-H$_3$Bpin** and 24% unknown iridium species in 10 min, and the formation of **10-Ir-H$_3$Bpin** proved the C_{sp}–B bond cleavage is facile. *cis*-Alkenylboronate (**A10-1**) was also observed.

Competence of isolated compounds in catalytic DHBTA

Chart 4 summarizes the results of catalytic DHBTA experiments that utilized various isolated (^{Me}PNP^{iPr})Ir compounds as pre-catalysts. The catalytic reactions were carried out in the fashion consistent with our other studies – the Ir compound was treated with 200 equiv. of HBpin, followed by 100 equiv. of the terminal alkyne (*i.e.*, 1 mol% Ir). When **10-Ir-H$_2$** was treated with excess HBpin, a yellow mixture of **10-Ir-HBpin** and **10-Ir-H$_3$Bpin** immediately formed before the addition of alkyne. Not surprisingly, essentially identical yields of **A1-Bpin** and hydrogenation side-product **A1-3** was observed when using **10-Ir-HBpin** and **10-Ir-H$_2$** as pre-catalysts. The use of **10-Ir-v-tol** did lead to the formation of **A1-Bpin**, but in a significantly smaller yield than with **10-Ir-HBpin** and **10-Ir-H$_2$**. In contrast, **10-Ir-Bpin$_2$** showed no DHBTA at all after the first 10 min and only gave 37% **A1-Bpin** after 3 h. The inertness of **10-Ir-Bpin$_2$** in the DHBTA correlated with its lack of reactivity in the stoichiometric reactions described above. In the two reactions with **A10-H**, **10-Ir-H$_2$** and **10-Ir-p-F$_3$tol** led to the same yield of **A10-Bpin** and the hydrogenation side-product **A10-1** (4-CF_3-C_6H_4-C_2H_5) at the 10 min and the 1 h mark.

On the basis of the stoichiometric and catalytic experiments the diboryl complexes analogous to **10-Ir-Bpin$_2$** and the vinylidene complexes analogous to **10-Ir-v-tol** can be firmly ruled out as intermediates in the DHBTA catalysis by (PNP)Ir complexes. Interestingly, this raises the question of whether the previously reported (SiNN)Ir catalysis actually requires **1-Ir-Bpin$_2$** as an intermediate or if it is merely an off-cycle precursor that can access the catalytic cycle rapidly enough.

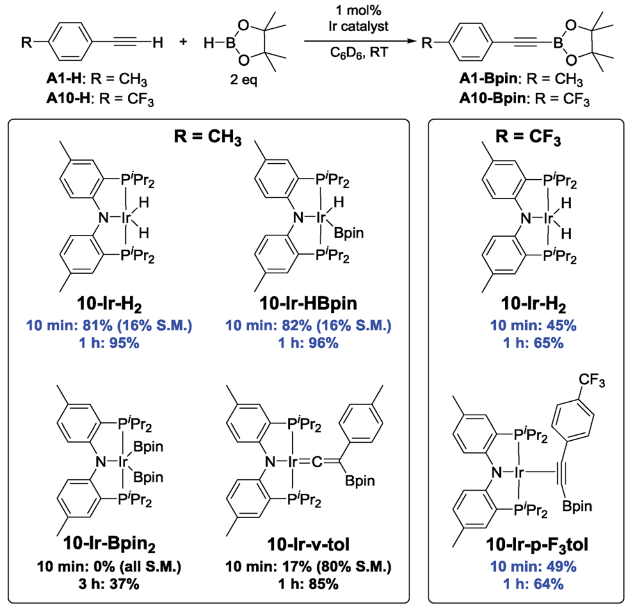

Chart 4 Catalytic results for DHBTA using various 10-Ir complexes.

Conclusions

Building on a recent report of successful dehydrogenative borylation of terminal alkynes (DHBTA) with a pincer iridium catalyst,[40] we examined a series of ligands structurally related to the successful SiNN ligand. Although most of the tested ligands failed to produce DHBTA products, we discovered that various PNP pincer ligands do result in active iridium DHBTA catalysts. Using the unsymmetric PNP-supported iridium complex **17-Ir-COE**, useful yields were obtained with 0.025% loading of catalyst, corresponding to thousands of turnovers. Good to excellent yields were obtained under mild conditions for aryl-, silyl-, and alkyl-substituted terminal alkynes, even propargyl derivatives and 1,6-enynes. Unlike the strict chemoselectivity in the (SiNN)Ir system, <10% hydrogenation products were observed as the main side-products in all the (PNP)Ir systems with arylacetylene substrates. This has not precluded isolation of alkynylboronate products in 70–82% yields on preparative scale.

Several iridium complexes of the symmetric PNP ligand **10** were synthesized and examined as potential intermediates in the catalytic cycle *via* testing in stoichiometric and catalytic reactions. The vinylidene (**10-Ir-v-tol**) and diboryl (**10-Ir-Bpin$_2$**) complexes reacted too slowly with either terminal alkynes or HBpin under the conditions of catalysis, which ruled them out of the catalytic cycle of the **10-Ir** system. The inactivity of **10-Ir-Bpin$_2$** is in contrast to the analogous **1-Ir-Bpin$_2$**[40] which suggests that a diboryl intermediate is not essential for successful DHBTA. On the other hand, the hydride boryl complex (**10-Ir-HBpin**) and the alkynylboronate π-complex (**10-Ir-p-F$_3$tol**) showed nearly identical performance to **10-Ir-H$_2$** indicating that they either are intermediates in the catalytic cycle or are connected to such *via* a low-barrier pathway. Although the full mechanistic picture remains uncertain, the presently reported results strongly suggest that a pincer ligand containing an amido donor is key to an active DHBTA catalyst with iridium. An intriguing possibility is that this is related to the facile migration of boryl from the metal to the amido nitrogen we recently discovered for **1-Ir-Bpin$_2$** and **1-Rh-Bpin$_2$**.[80]

Acknowledgements

We are grateful for the support of this research by the US National Science Foundation (grant CHE-1310007 to O. V. O.), the Welch Foundation (grant A-1717 to O. V. O.), and Fundamental Research Funds for the Central Universities of China (Grant No. AUGA5710013115 to J. Z.). We are also grateful to Ms. Linda Redd for editorial assistance.

Notes and references

1 J. F. Hartwig, *Chem. Soc. Rev.*, 2011, **40**, 1992.
2 I. A. I. Mkhalid, J. H. Barnard, T. B. Marder, J. M. Murphy and J. F. Hartwig, *Chem. Rev.*, 2010, **110**, 890.
3 J. H. Brewster and E.-I. Negishi, *Science*, 1980, **207**, 44.
4 Y. Kondo, D. Garcia-Cuadrado, J. F. Hartwig, N. K. Boaen, N. L. Wagner and M. A. Hillmyer, *J. Am. Chem. Soc.*, 2002, **124**, 1164.
5 J. Shin, S. M. Jensen, J. Ju, S. Lee, Z. Xue, S. K. Noh and C. Bae, *Macromolecules*, 2007, **40**, 8600.
6 R. E. Maleczka Jr, F. Shi, D. Holmes and M. R. Smith III, *J. Am. Chem. Soc.*, 2003, **125**, 7792.
7 A. Suzuki, *Angew. Chem., Int. Ed.*, 2011, **50**, 6722.
8 E. M. Beck, R. Hatley and M. J. Gaunt, *Angew. Chem., Int. Ed.*, 2008, **47**, 3004.
9 A. D. Finke and J. S. Moore, *Org. Lett.*, 2008, **10**, 4851.
10 H. Chen, S. Schlecht, T. C. Semple and J. F. Hartwig, *Science*, 2000, **287**, 1995.
11 J. M. Murphy, J. D. Lawrence, K. Kawamura, C. Incarvito and J. F. Hartwig, *J. Am. Chem. Soc.*, 2006, **128**, 13684.
12 H. Chen and J. F. Hartwig, *Angew. Chem., Int. Ed.*, 1999, **38**, 3391.
13 T. Ishiyama, J. Takagi, K. Ishida, N. Miyaura, N. R. Anastasi and J. F. Hartwig, *J. Am. Chem. Soc.*, 2002, **124**, 390.
14 J.-Y. Cho, M. K. Tse, D. Holmes, R. E. Maleczka Jr and M. R. Smith III, *Science*, 2002, **295**, 305.
15 J. M. Brown and G. C. Lloyd-Jones, *J. Am. Chem. Soc.*, 1994, **116**, 866.
16 R. B. Coapes, F. E. S. Souza, R. L. Thomas, J. J. Hall and T. B. Marder, *Chem. Commun.*, 2003, 614.
17 T. Ishiyama, K. Ishida, J. Takagi and N. Miyaura, *Chem. Lett.*, 2001, **30**, 1082.
18 V. J. Olsson and K. J. Szabó, *Angew. Chem., Int. Ed.*, 2007, **46**, 6891.
19 Q. Li, C. W. Liskey and J. F. Hartwig, *J. Am. Chem. Soc.*, 2014, **136**, 8755.
20 S. H. Cho and J. F. Hartwig, *Chem. Sci.*, 2014, **5**, 694.
21 B. Ghaffari, S. M. Preshlock, D. L. Plattner, R. J. Staples, P. E. Maligres, S. W. Krska, R. E. Maleczka Jr and M. R. Smith III, *J. Am. Chem. Soc.*, 2014, **136**, 14345.
22 S. M. Preshlock, B. Ghaffari, P. E. Maligres, S. W. Krska, R. E. Maleczka Jr and M. R. Smith III, *J. Am. Chem. Soc.*, 2013, **135**, 7572.
23 D. Ogawa, J. Li, M. Suetsugu, J. Jiao, M. Iwasaki and Y. Nishihara, *Tetrahedron Lett.*, 2013, **54**, 518.
24 V. Gandon, D. Leca, T. Aechtner, K. P. C. Vollhardt, M. Malacria and C. Aubert, *Org. Lett.*, 2004, **6**, 3405.
25 J. Huang, S. J. F. Macdonald and J. P. A. Harrity, *Chem. Commun.*, 2009, 436.
26 J. Barluenga, P. Barrio, L. Riesgo, L. A. López and M. Tomás, *J. Am. Chem. Soc.*, 2007, **129**, 14422.
27 L. Deloux, E. Skrzypczak-Jankun, B. V. Cheesman, M. Srebnik and M. Sabat, *J. Am. Chem. Soc.*, 1994, **116**, 10302.
28 J. Renaud, C.-D. Graf and L. Oberer, *Angew. Chem., Int. Ed.*, 2000, **39**, 3101.
29 M. M. Hussain, H. Li, N. Hussain, M. Ureña, P. J. Carroll and P. J. Walsh, *J. Am. Chem. Soc.*, 2009, **131**, 6516.
30 A.-L. Auvinet and J. P. A. Harrity, *Angew. Chem., Int. Ed.*, 2011, **50**, 2769.
31 M. M. Hussain, J. H. Toribio, P. J. Carroll and P. J. Walsh, *Angew. Chem., Int. Ed.*, 2011, **50**, 6337.
32 Y. Nishihara, Y. Okada, J. Jiao, M. Suetsugu, M.-T. Lan, M. Kinoshita, M. Iwasaki and K. Takagi, *Angew. Chem., Int. Ed.*, 2011, **50**, 8660.
33 H. C. Brown, N. G. Bhat and M. Srebnik, *Tetrahedron Lett.*, 1988, **29**, 2631.
34 J.-R. Hu, L.-H. Liu, X. Hu and H.-D. Ye, *Tetrahedron*, 2014, **70**, 5815.
35 J. R. Lawson, E. R. Clark, I. A. Cade, S. A. Solomon and M. J. Ingleson, *Angew. Chem., Int. Ed.*, 2013, **52**, 7518.
36 I. Beletskaya and A. Pelter, *Tetrahedron*, 1997, **53**, 4957.
37 B. M. Trost and Z. T. Ball, *Synthesis*, 2005, **6**, 853.
38 I. N. Michaelides and D. J. Dixon, *Angew. Chem., Int. Ed.*, 2013, **52**, 806.
39 For information on the chemistry of pincer ligands in general, see: (*a*) M. E. van der Boom and D. Milstein, *Chem. Rev.*, 2003, **103**, 1759; (*b*) *The Chemistry of Pincer Compounds*, ed. D. Morales-Morales, and C. Jensen, Elsevier, Amsterdam, 2007; (*c*) J. Choi, A. H. R. MacArthur, M. Brookhart and A. S. Goldman, *Chem. Rev.*, 2011, **111**, 1761.
40 C.-I. Lee, J. Zhou and O. V. Ozerov, *J. Am. Chem. Soc.*, 2013, **135**, 3560.
41 T. Tsuchimoto, H. Utsugi, T. Sugiura and S. Horio, *Adv. Synth. Catal.*, 2015, **357**, 77.
42 C. J. Pell and O. V. Ozerov, *Inorg. Chem. Front.*, 2015, **2**, 720.
43 (*a*) J. Choi, A. H. R. MacArthur, M. Brookhart and A. S. Goldman, *Chem. Rev.*, 2011, **111**, 1761; (*b*) G. E. Dobereiner, J. Yuan, R. R. Schrock, A. S. Goldman and J. D. Hackenberg, *J. Am. Chem. Soc.*, 2013, **135**, 12572.
44 L. Fan, S. Parkin and O. V. Ozerov, *J. Am. Chem. Soc.*, 2005, **127**, 16772.
45 Y. Zhu, L. Fan, C.-H. Chen, S. R. Finnell, B. M. Foxman and O. V. Ozerov, *Organometallics*, 2007, **26**, 6701.

46 (*a*) M. T. Whited, Y. Zhu, S. D. Timpa, C.-H. Chen, B. M. Foxman, O. V. Ozerov and R. H. Grubbs, *Organometallics*, 2009, **28**, 4560; (*b*) M. T. Whited and R. H. Grubbs, *Acc. Chem. Res.*, 2009, **42**, 1607.
47 D. Liu, Y. Luo, W. Gao and D. Cui, *Organometallics*, 2010, **29**, 1916.
48 J. C. Peters, S. B. Harkins, S. D. Brown and M. W. Day, *Inorg. Chem.*, 2001, **40**, 5083.
49 D. E. Herbert and O. V. Ozerov, *Organometallics*, 2011, **30**, 6641.
50 J. J. Davidson, J. C. DeMott, C. Douvris, C. M. Fafard, N. Bhuvanesh, C.-H. Chen, D. E. Herbert, C.-I. Lee, B. J. McCulloch, B. M. Foxman and O. V. Ozerov, *Inorg. Chem.*, 2015, **54**, 2916.
51 M. Gupta, C. Hagen, W. C. Kaska, R. E. Cramer and C. M. Jensen, *J. Am. Chem. Soc.*, 1997, **119**, 840.
52 I. Göttker-Schnetmann, P. S. White and M. Brookhart, *Organometallics*, 2004, **23**, 1766.
53 F. Liu, E. B. Pak, B. Singh, C. M. Jensen and A. S. Goldman, *J. Am. Chem. Soc.*, 1999, **121**, 4086.
54 A. C. Sykes, P. White and M. Brookhart, *Organometallics*, 2006, **25**, 1664.
55 R. Ahuja, M. Brookhart, A. S. Goldman, Z. Huang, and A. R. Macarthur, WO 2007008847 A2, 18 Jan 2007.
56 D. Morales-Morales, R. Redón, C. Yung and C. M. Jensen, *Inorg. Chim. Acta*, 2004, **357**, 2953.
57 L. P. Press, B. J. McCulloch and O. V. Ozerov, manuscript in preparation.
58 T. Ishiyama, J. Takagi, J. F. Hartwig and N. Miyaura, *Angew. Chem., Int. Ed.*, 2002, **41**, 3056.
59 See ESI† for details.
60 J. D. Masuda, K. C. Jantunen, O. V. Ozerov, K. J. T. Noonan, D. P. Gates, B. L. Scott and J. L. Kiplinger, *J. Am. Chem. Soc.*, 2008, **130**, 2408.
61 R. B. Lansing, K. I. Goldberg and R. A. Kemp, *Dalton Trans.*, 2011, 8950.
62 E. Calimano and T. D. Tilley, *Dalton Trans.*, 2010, 9250.
63 R. H. Crabtree, *Chem. Rev.*, 2012, **112**, 1536.
64 T. J. Hebden, M. C. Denney, V. Pons, P. M. B. Piccoli, T. F. Koetzle, A. J. Schultz, W. Kaminsky, K. I. Goldberg and D. M. Heinekey, *J. Am. Chem. Soc.*, 2008, **130**, 10812.
65 W. Weng, C. Guo, R. Celenligil-Cetin, B. M. Foxman and O. V. Ozerov, *Chem. Commun.*, 2006, 197.
66 R. Ghosh, X. Zhang, P. Achord, T. J. Emge, K. Krogh-Jespersen and A. S. Goldman, *J. Am. Chem. Soc.*, 2007, **129**, 853.
67 N. Phadke and M. Findlater, *Organometallics*, 2013, **33**, 16.
68 M. I. Bruce, *Chem. Rev.*, 1991, **91**, 197.
69 M. A. Esteruelas, A. M. López, M. Mora and E. Oñate, *Organometallics*, 2012, **31**, 2965.
70 D. A. Ortmann, B. Weberndörfer, K. Ilg, M. Laubender and H. Werner, *Organometallics*, 2002, **21**, 2369.
71 P. Steinert and H. Werner, *Chem. Ber.*, 1997, **130**, 1591.
72 J. L. Templeton, *Adv. Organomet. Chem.*, 1989, **29**, 1.
73 J. F. Riehl, Y. Jean, O. Eisenstein and M. Pelissier, *Organometallics*, 1992, **11**, 729.
74 W. H. Lam, S. Shimada, A. S. Batsanov, Z. Lin, T. B. Marder, J. A. Cowan, J. A. K. Howard, S. A. Mason and G. J. McIntyre, *Organometallics*, 2003, **22**, 4557.
75 ORTEP plots were created using Ortep-3 for Windows. L. Farugia, *J. Appl. Crystallogr.*, 1997, **30**, 565.
76 M. D. Fryzuk, L. Huang, N. T. McManus, P. Paglia, S. J. Rettig and G. S. White, *Organometallics*, 1992, **11**, 2979.
77 D. B. Grotjahn, J. M. Hoerter and J. L. Hubbard, *J. Am. Chem. Soc.*, 2004, **126**, 8866.
78 N. Grüger, H. Wadepohl and L. H. Gade, *Eur. J. Inorg. Chem.*, 2013, **30**, 5358.
79 R. H. Crabtree, *The Organometallic Chemistry of the Transition Metals*, Wiley, 2005.
80 C.-I. Lee, N. A. Hirscher, J. Zhou, N. Bhuvanesh and O. V. Ozerov, *Organometallics*, 2015, **34**, 3099.

